

The Extreme Wind Events in the Ross Island Region of Antarctica

NICHOLAS J. WEBER^a

Antarctic Meteorological Research Center, Space Science and Engineering Center, and Department of Atmospheric and Oceanic Sciences, University of Wisconsin–Madison, Madison, Wisconsin

MATTHEW A. LAZZARA

Antarctic Meteorological Research Center, Space Science and Engineering Center, University of Wisconsin–Madison, and Department of Physical Sciences, School of Arts and Sciences, Madison Area Technical College, Madison, Wisconsin

LINDA M. KELLER

Antarctic Meteorological Research Center, Space Science and Engineering Center, and Department of Atmospheric and Oceanic Sciences, University of Wisconsin–Madison, Madison, Wisconsin


JOHN J. CASSANO

Cooperative Institute for Research in Environmental Sciences, and Department of Atmospheric and Oceanic Sciences, University of Colorado, Boulder, Colorado

(Manuscript received 21 September 2015, in final form 13 April 2016)

ABSTRACT

Numerous incidents of structural damage at the U.S. Antarctic Program's (USAP) McMurdo Station due to extreme wind events (EWEs) have been reported over the past decade. Utilizing nearly 20 yr (~1992–2013) of University of Wisconsin automatic weather station (AWS) data from three different stations in the Ross Island region (Pegasus North, Pegasus South, and Willie Field), statistical analysis shows no significant trends in EWE frequency, intensity, or duration. EWEs more frequently occur during the transition seasons. To assess the dynamical environment of these EWEs, Antarctic Mesoscale Prediction System (AMPS) forecast back trajectories are computed and analyzed in conjunction with several other AMPS fields for the strongest events at McMurdo Station. The synoptic analysis reveals that McMurdo Station EWEs are nearly always associated with strong southerly flow due to an approaching Ross Sea cyclone and an upper-level trough around Cape Adare. A Ross Ice Shelf air stream (RAS) environment is created with enhanced barrier winds along the Transantarctic Mountains, downslope winds in the lee of the glaciers and local topography, and a tip jet effect around Ross Island. The position and intensity of these Ross Sea cyclones are most influenced by the occurrence of a central Pacific ENSO event, which causes the upper-level trough to move westward. An approaching surface cyclone would then be in position to trigger an event, depending on how the wind direction and speed impinges on the complex topography around McMurdo Station.

 Denotes Open Access content.

^aCurrent affiliation: Department of Atmospheric Sciences, University of Washington, Seattle, Washington.

Corresponding author address: Linda M. Keller, Antarctic Meteorological Research Center, Space Science and Engineering Center, University of Wisconsin–Madison, 1225 West Dayton St., Madison, WI 53706.
E-mail: lmkeller@wisc.edu

1. Introduction

There have been numerous studies of strong wind events (SWEs) throughout the Antarctic continent. East Antarctica is especially susceptible to strong or extreme wind events because of the steeply sloping topography and the presence of intense synoptic-scale cyclones. A modeling analysis of SWEs using perpetual July mode at the Australian coastal site Casey in East Antarctica (Fig. 1a) showed that synoptic winds (cyclones) and katabatic flow are equally present during the development of

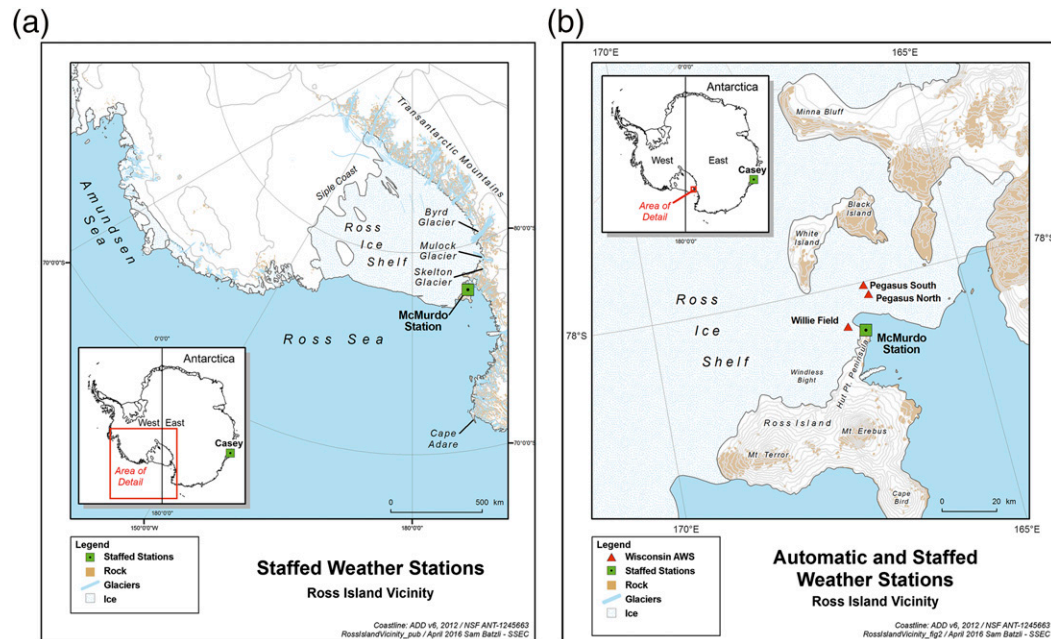


FIG. 1. Map inset of the (a) Ross Ice Shelf and (b) Ross Island region indicating staffed stations, AWSs, and important topographical features.

severe winds, though their average wind vectors are nearly perpendicular to each other in this region (i.e., the katabatic winds do not enhance the synoptic flow; [Murphy and Simmonds 1993](#)). Further investigation into East Antarctic SWEs (utilizing models and station observations for December 1999) revealed that, while downslope winds can certainly add to the severity of the wind event, extratropical cyclones are a prevalent feature of these SWEs and are the dominant forcing ([Murphy 2003](#)). [Turner et al. \(2009\)](#) emphasize that the katabatic contribution to East Antarctic SWEs is crucially dependent on the specific interaction between the synoptic regime and the downslope flow, or the position of cyclones relative to topographic features such as glaciers or valleys.

SWEs in many studies have been defined by categories of the Beaufort scale. [Chenoli et al. \(2012\)](#) used the Beaufort scale of 6 (11.3 m s^{-1}) based on the blowing snow threshold of 10 m s^{-1} from [King and Turner \(1997\)](#) and [Schwerdtfeger \(1984\)](#) and the frequency distribution of 10-min average wind speeds for McMurdo Station to examine strong wind events in the McMurdo area for the period 1979–2005, while [Turner et al. \(2009\)](#) used gale (17.2 m s^{-1}) or storm (24.5 m s^{-1}) force scales for plateau and coastal SWEs, respectively. The Turner et al. study used data from around the Antarctic continent for the period 1954–2006.

The drastically different topographical features—and the corresponding, varied responses of different flow regimes ([Seefeldt et al. 2003](#))—in the Ross Island region

([Fig. 1b](#)) warrant a separate investigation of the dynamical forcings behind McMurdo Sound severe winds. Wind events in the McMurdo Station and Ross Island region in the Antarctic pose a major threat not only to structures in McMurdo Station and Scott Base, but also to flight operations and safety. Extreme winds, such as those observed in the previously studied McMurdo Station event on 15–16 May 2004 ([Powers 2007](#); [Steinhoff et al. 2008](#)), can cause significant damage to permanent structures and equipment, while winds as weak as 7 m s^{-1} can be a travel hazard because of blowing snow ([Bromwich 1988](#); [Holmes et al. 2000](#); [Knuth et al. 2010](#)).

Recent research has examined McMurdo area SWEs and their associated wind regimes in the Ross Island region with a focus on in situ observations ([Holmes et al. 2000](#)), satellite observations ([Bromwich 1989](#)), and, most commonly, modeling ([Seefeldt et al. 2003](#); [Powers 2007](#); [Steinhoff et al. 2008](#); [O'Connor et al. 1994](#); [Monaghan et al. 2005](#)). Owing to the paucity of ground-based observations, modeling studies are an important means of depicting the larger-scale features associated with the SWEs. The complex, small-scale features that are present during an SWE, due to the topography of the area, can only be represented by regional mesoscale models.

Multiple dominant dynamical features have been suspected as initiating SWEs in the Ross Island region: katabatic winds ([Bromwich 1989](#); [Parish and Bromwich 1998](#)), barrier winds along the Transantarctic Mountains

(O'Connor et al. 1994), cyclonic events in the vicinity of Ross Island and McMurdo Sound (Carrasco and Bromwich 1993; Powers 2007; Steinhoff et al. 2008), hydraulic jumps, and potentially downslope winds accelerated by gravity waves (Steinhoff et al. 2008). The consensus is that more than one of these mechanisms occurs during an SWE. One key difference between Ross Island SWEs and the aforementioned events in East Antarctica is the prominence of the Ross Ice Shelf air stream (RAS) in the Ross Ice Shelf wind regime, of which barrier flow is a major component.

A recent climatology of McMurdo Station SWEs by Chenoli et al. (2012) revealed that, although the overall trend in the number of SWEs from 1979 to 2005 is insignificant, a bimodal distribution in the wind direction exists during these events. This bimodal distribution is consistent with Holmes et al. (2000) in that weaker SWEs tend to get blocked by terrain and flow around from the northeast, while stronger events can overcome the barriers and result in a southerly SWE (Chenoli et al. 2012). The latter of these two SWE types—characterized by stronger winds and southerly flow over terrain—is consistently accompanied by deep Ross Ice Shelf depressions (Chenoli et al. 2012).

This study aims to expand upon the prior research by examining both the climatology and dynamical environment of the highest-intensity (storm force or greater on the Beaufort scale) extreme wind events (EWEs) with the greatest possibility of destruction of facilities at staffed stations. Understanding EWEs is of great importance to Antarctic forecasters, as these high-profile wind events are mostly responsible for both structural damage at stations and perilous travel conditions for ground and aviation operations. The purpose of this study is to discover if there are any significant dynamical or climatological differences between EWEs (Beaufort-scale storm force, 24.7 m s^{-1}) and SWEs (Beaufort-scale category 6, 11.3 m s^{-1}), and which components of the dynamical environment are most prominent in these extreme cases. Furthermore, the characteristics of top-tier wind events are of great value to the engineering community, as this knowledge can be implemented in future construction projects in the Ross Island vicinity. The above insights will be gained using in situ observations from McMurdo Station, University of Wisconsin automatic weather station (AWS) data and other observational data from nearby stations, and Antarctic Mesoscale Prediction System (AMPS) forecast data. Details regarding the data and analysis methods will be discussed in section 2. The synoptic situation, as well as results of the statistical analysis, will be discussed in section 3, and the dynamical study is presented in section 4. Closing remarks will then be given in sections 5 and 6.

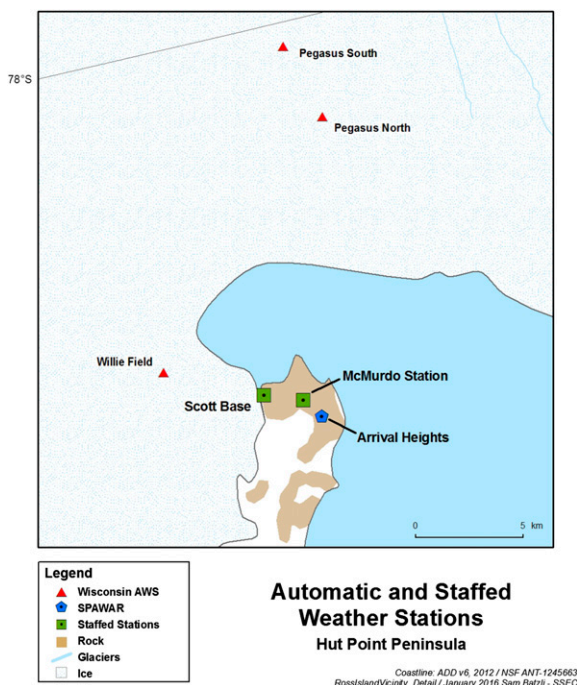


FIG. 2. Detail of Ross Island area.

2. Data and methods

An intricate relationship exists between the wind regime and the orography in the Ross Island vicinity (Fig. 2). Much of the spatial and temporal variation in the Ross Island airflow is explained by the modulation of the large-scale wind patterns by the local static stability and complex topography (Seefeldt et al. 2003; O'Connor et al. 1994; Adams 2005; Chenoli et al. 2015). Ross Island, on the east side of McMurdo Sound, is roughly 75 km long and 35 km wide and encompasses both Mount Erebus and Mount Terror, two peaks that rise from sea level to over 3000 m (Fig. 1b). The staffed Antarctic stations of McMurdo and Scott Base lie on the very end of Hut Point Peninsula, a 20-km extension of Ross Island. On the south edge of the island, the 900-km-long Ross Ice Shelf begins its vast extent into the Antarctic continent. Additional orographic features in the Ross Island region include Minna Bluff, an 800-m-high ridge that sits 80 km to the south of Ross Island; Black Island and White Island, two features with elevations of 1000 and 800 m, respectively, 30 km south of Ross Island; and the Transantarctic Mountains 80 km west of Ross Island, running from the Ross Sea along the western edge of the Ross Ice Shelf.

The wind in the Ross Island vicinity is highly dependent on the large-scale flow patterns over the entire Ross Ice Shelf, which can often be characterized by a

TABLE 1. Wind speed and direction instrumentation for McMurdo Station and the Pegasus North, Pegasus South, and Willie Field AWSs.

Instrument	Sensor	Location	Resolution	Range
Wind speed	R. M. Young 01503	Pegasus North Pegasus South Willie Field	0.195 m s^{-1}	$1\text{--}100 \text{ m s}^{-1}$
Wind direction	Bendix/Belfort 10 000-ohm potentiometer	McMurdo Station All	0.250 m s^{-1} 1.5°	$2\text{--}63 \text{ m s}^{-1}$ $0^\circ\text{--}355^\circ$

semipermanent wind regime called the Ross Ice Shelf air stream flowing parallel to the Transantarctic Mountains from the Siple Coast (Fig. 1a) up through the Ross Island region (Parish et al. 2006; Seefeldt et al. 2007; Steinhoff et al. 2009; Nigro and Cassano 2014a; Coggins and McDonald 2015). The RAS flow pattern is a composite of several different features, including katabatic winds, barrier winds, and synoptic flow (i.e., cyclones and anticyclones), all of which interact with each other (Nigro and Cassano 2014b). O'Connor et al. (1994) noted that geostrophic flow running perpendicular to the Transantarctic Mountains—such as that forced by an ice shelf cyclone—creates a dominant barrier flow that results in strong southerly flow in the Ross Island region. While attempting to characterize the dominant regimes over the Ross Ice Shelf as katabatic, barrier, or weak flow, Seefeldt et al. (2007) concluded that these wind regimes alone classify under half of the total summer hours over the shelf, implying that most of the flow in the region can be characterized by a combination of these regimes in conjunction with synoptic disturbances. Nigro and Cassano (2014b) found that the semipermanent elevated baroclinic zone at the edge of the East Antarctic plateau provides forcing for the barrier-parallel flow that characterizes the RAS. Unsurprisingly, changes in the intensity of the RAS and its contributing flow regimes have a significant impact on the severity of the wind in the Ross Ice Shelf region.

For the statistical EWE analysis, quality-controlled University of Wisconsin AWS data from the Pegasus North, Pegasus South, and Willie Field sites are used (Fig. 2) (Lazzara et al. 2012). These stations are used because of their proximity to the staffed McMurdo Station and their long, quality-controlled records. The AWS observations are recorded every 10 min with the

wind sensors outlined in Table 1. The threshold for EWE calculations is 24.7 m s^{-1} , which is well above the 95th percentile wind speed for each station and represents the threshold for a Beaufort storm scale of 10 or what is known as a condition 2 (Table 2) weather event at McMurdo Station. For the AWS data, an EWE exists when over half of the 10-min observations in a 3-h interval are over the threshold; when adjacent 3-h intervals meet this criterion, they are combined into a single event. Values recorded for these events include maximum wind speed, average resultant wind speed, resultant wind direction, starting date, ending date, and duration. EWEs are computed from 1992 to 2013, but all three stations consistently recorded data only through 2009. Pegasus North was the only operational station of the three from 2011 to 2013, and 2014 has been eliminated as a result of several months of missing data in the austral winter. McMurdo Station data are omitted from the statistical analysis because of the inconsistent reporting in winter months. McMurdo Station data before the late 1990s were not quality controlled and were used mainly for aviation operations. The Space and Naval Warfare Systems Command (SPAWAR) has been tasked with forecasting since then and has been working to provide quality control for the data to allow it to be used for climate studies.

To examine the synoptic conditions accompanying the occurrence of EWEs, the top 12 events based on maximum wind speed at McMurdo Station between 2001 and 2013 were chosen so they can be analyzed with the AMPS model (which was developed in 2000; Powers et al. 2012). Data for McMurdo Station were chosen for the synoptic analysis since that is where significant damage has occurred during these extreme events and where aviation operations are impacted. The selection

TABLE 2. The three weather condition levels for McMurdo Station, categorized by their wind speed (kt; $1 \text{ kt} = 0.51 \text{ m s}^{-1}$), wind chill temperature, and visibility thresholds. For each condition, the station has different policies regarding travel and outdoor activity.

Condition	Wind speed (kt)	Wind chill temp (F)	Visibility	Travel restrictions
3	<48	> -75°	> $1/4 \text{ mi}$	None
2	48–55	From -75° to -100°	From $1/4 \text{ mi}$ to 100 ft	Only enclosed vehicles with radios can leave
1	>55	< -100°	<100 ft	All personnel must stay indoors

TABLE 3. The start date, maximum speed, average speed, resultant direction (vector average), and duration of the top 12 McMurdo Station EWEs. Note that the May 2004 EWE data were obtained from the SPAWAR Arrival Heights AWS data. The winds are considerably stronger because Arrival Heights is at a higher, more exposed location inland above McMurdo Station.

Start date	Max speed (m s^{-1})	Avg speed (m s^{-1})	Direction	Duration (h)
12 Dec 2001	21.10	18.06	167.02°	18
21 Aug 2002	21.60	16.68	183.38°	9
23 May 2003	20.60	18.87	174.03°	6
3 Sep 2003	27.20	19.35	154.79°	15
1 Dec 2003	22.10	18.50	173.29°	9
15 May 2004	48.30	29.10	160.60°	9
29 Jun 2005	25.20	21.58	183.77°	9
20 Sep 2006	20.60	18.87	170.00°	6
12 Apr 2009	26.20	21.38	196.59°	12
19 Apr 2009	25.20	20.80	183.89°	9
8 May 2012	26.60	22.90	188.40°	6
21 May 2012	22.60	18.88	181.00°	12

of events is also corroborated by the AWSs listed above. As noted above, more recent (i.e., AMPS era) McMurdo Station data do not have as many of the issues with quality and reporting consistency because the observing/forecasting operation has been actively quality controlling the data.

In situ wind observations from McMurdo Station between 2001 and 2013 were recorded every 3 h (with the instrumentation in Table 1). The wind speeds at McMurdo Station exhibit considerably weaker wind speeds than from nearby AWSs; this is likely due to the frictional interference of the town structures with the strong winds (A. Cayette 2015, personal communication). A comparison with Scott Base data for the events chosen showed that Scott Base wind speeds were generally $3\text{--}5\text{ m s}^{-1}$ higher, although some cases were actually lower than the McMurdo Station wind speeds. Using the condition 2 (24.7 m s^{-1}) threshold resulted in only six EWEs being reported. To get a larger sample size, the threshold was changed to 15 m s^{-1} . This threshold is still above the 95th percentile for McMurdo Station wind speeds. An EWE is identified in the McMurdo Station data if three or more consecutive 3-hourly wind speed observations exceed the modified EWE threshold. Three consecutive observations exceeding the 15 m s^{-1} threshold results in a 6-h-long EWE, as only 6 h have passed between the first and last observations. Likewise, four consecutive observations result in a 9-h EWE and five consecutive observations yield a 12-h event, etc. From the events that meet these criteria, the top 11 are chosen based on their maximum wind speed values. In addition to these top 11 events, the historic EWE from 15 to 16 May 2004 (Powers 2007; Steinhoff et al. 2008) is also included; this event is not reported in the McMurdo Station data (or in the data of many of the surrounding AWS) because the winds were so strong during this event that the stations' anemometers

were destroyed or damaged. The data used to represent this event are from the SPAWAR Arrival Heights McMurdo area wind sensor network station (15-min data), and the EWE is quantified using the same methods as were used with the 10-min AWS data in the statistical analysis. As an example of how the Arrival Heights wind data compare to the McMurdo Station wind data, for the event on 29 June 2005, the maximum wind speed for McMurdo Station was 25.2 m s^{-1} and at Arrival Heights the maximum was 35.4 m s^{-1} . The resultant wind speed and direction at McMurdo Station were 21.6 m s^{-1} from 184° while at Arrival Heights they were 21.9 m s^{-1} from 152° . The resultant wind speed and direction are calculated by decomposing the vector wind into its zonal u and meridional v components, averaging the components, and then recombining the averaged components to get the average vector or resultant wind. The top 12 EWE events chosen for the additional dynamical analysis are listed in Table 3.

Forecast back trajectories are computed for these 12 McMurdo Station EWE cases using the Hybrid Single-Particle Lagrangian Integrated Trajectory model (HYSPLIT) from the National Oceanic and Atmospheric Administration's (NOAA) Air Resources Laboratory forced with AMPS model data. While this is not the first time HYSPLIT back trajectories have been used in an Antarctic setting (Markle et al. 2012), most other studies have employed the NCEP–NCAR reanalyses dataset. Here, AMPS forecasts are used from 2001 to 2013 during which time the model evolved from the Fifth-generation Pennsylvania State University–NCAR Mesoscale Model (MM5) to the Weather Research and Forecasting (WRF) Model in 2006. The D2 window [nested AMPS domain covering the entire Antarctic continent; see Powers (2007), their Fig. 1a] used in this study started as a 30-km grid in 2000, became a 20-km grid in 2005, and finally a

TABLE 4. Period of operation for AWSs.

Station	Period of operation	No. of events
Pegasus North	1992–2013	62
Pegasus South	1992–2009	26
Willie Field	1992–2009	2

15-km grid from 2008 onward (Powers et al. 2012). The AMPS model, which has been optimized for use as a forecast model in the Antarctic (Powers et al. 2012) and has had several studies performed on its forecasting and diagnostic abilities (Bromwich et al. 2003, 2005; Guo et al. 2003), is used instead of a global reanalysis model such as ERA-Interim because it has a higher resolution, which can more accurately depict the terrain along the Transantarctic Mountains as well as the complex topography around McMurdo Station. A forecast back trajectory for an EWE is initialized 3 days into the AMPS forecast at McMurdo Station at the time of the EWE onset and computed backward through the zero forecast hour (some AMPS forecasts were shorter than 3 days in 2001 and 2002). These forecast back trajectories, in conjunction with other AMPS fields, are analyzed to determine where EWE parcels come from at different levels and what kinds of synoptic scenarios are favorable for the development of extreme winds.

3. Statistical analysis

Wind data from the Pegasus North, Pegasus South, and Willie Field AWSs are analyzed from 1992 to 2009. Throughout this time period (1992–2009), 46 EWEs were identified for Pegasus North, 26 for Pegasus South, and only 2 for Willie Field. Pegasus North operated for four more years after the other two AWS, and 16 more EWEs were identified at Pegasus North during 2010–13 (Table 4). The scarcity of EWEs at Willie Field is not unexpected, as the average monthly maximum wind speed at the station is consistently lower (by $\sim 6 \text{ m s}^{-1}$) than that at Pegasus North and Pegasus South; this difference appears in the average yearly maximum as well, as Willie Field's average is just under 8 m s^{-1} lower than that of Pegasus North and Pegasus South (C. Costanza 2015, personal communication). The difference in wind speeds has remained constant even though wind sensors have been replaced over the course of the observing period. As a result, wind speeds at Willie Field are, in most cases, just below the threshold of an EWE at an AWS. The complex flow patterns around the topography of Black and White Islands can create localized high wind speeds at Pegasus North and Pegasus South stations (Holmes et al. 2000), where maximum wind speeds

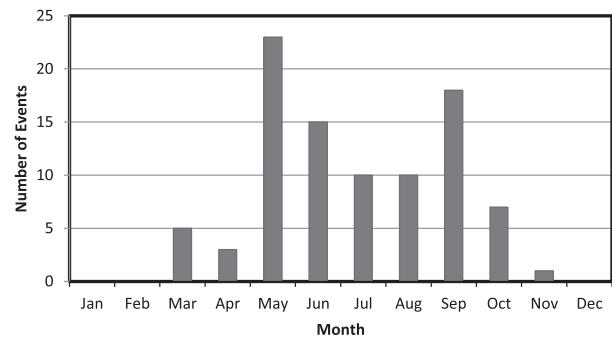


FIG. 3. The number of EWEs at the Pegasus North, Pegasus South, and Willie Field AWSs (duplicates combined) during each month, summed from 1992 to 2013.

are higher than those of nearby AWS sites (Keller et al. 1996, 1997). In addition, modeling studies show a high pressure area developing to the south of Ross Island as wind speeds increase from the south (Seefeldt et al. 2003, Adams 2005; Chenoli et al. 2012, 2015). It is possible that the edge of this high pressure area, and the lighter winds associated with it, extends to the west far enough to affect the wind speeds at Willie Field. These observations help explain why the Willie Field AWS experienced a negligible number of EWEs compared to the two Pegasus AWS sites.

The monthly distribution of the EWEs (Fig. 3) reveals that most of the EWEs occur during the transition seasons between the austral summer and winter as the peaks in EWE counts occur in May and September, with some events during June–August and no events at the AWS stations from December to February. Coggins and McDonald (2015) show that the shift of the Amundsen Sea low (ASL) in summer moves the cyclone activity away from the Ross Sea region, which decreases the likelihood of RAS events. The austral summer minimum in EWEs is consistent with the SWE distribution created by Chenoli et al. (2012), although the split peaks between spring and fall—rather than a midwinter peak—constitute a disparity between the current results and those of Chenoli et al. (2012). The peaks in EWE frequency during the spring and fall may be a manifestation of the semiannual oscillation (SAO), or the periodic expansion/contraction of the circumpolar trough, which creates deeper and more southerly low pressure systems during the austral spring and fall (Cohen et al. 2013). The strong connection between EWEs and low pressure systems is further detailed in section 4.

Figure 4 shows the wind roses for the EWEs at each station, indicating predominantly southerly flow during these events. This, too, is consistent with the Chenoli et al. (2012) bimodal wind direction classification of SWEs, wherein only the strongest events (EWEs) have

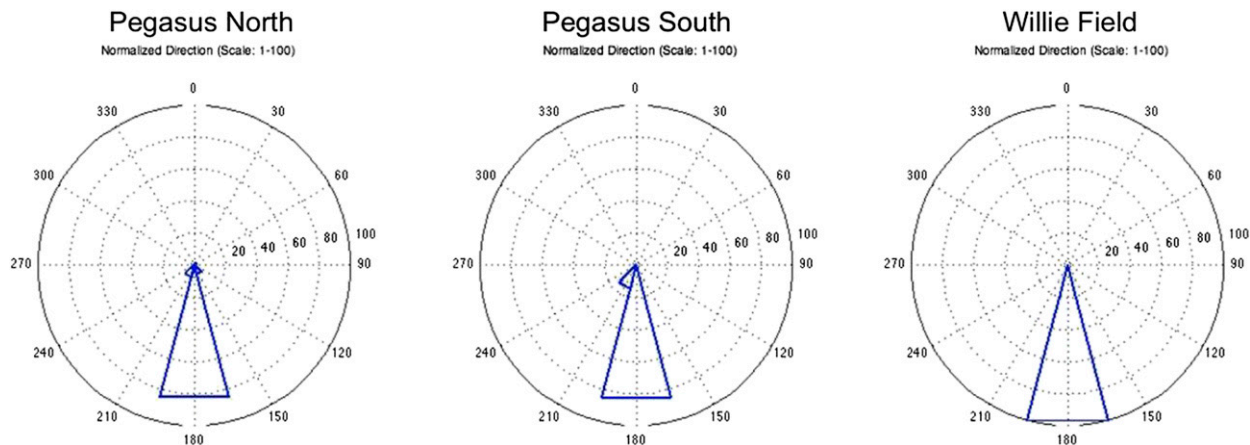


FIG. 4. Normalized direction wind roses for the EWE winds at Pegasus North, Pegasus South, and Willie Field.

sufficient energy to overcome topographical barriers, resulting in southerly flow at Ross Island. The “normalized” direction is the percent of the time in a given collection of data that the wind is coming from that direction.

Climatologically, the trends in EWE count (Fig. 5) for Pegasus North for 1992–2013 and Pegasus South for 1992–2009 are slightly positive but statistically insignificant. The EWE count at Willie Field is trendless, as there are only two events. Similarly insignificant trends were found for the EWE duration and intensity at these stations. While the AWS data used for this analysis are quality controlled, gaps in the data due to station malfunctions and instrumentation failures do exert a bias on the results, particularly during the first half of the 1992–2013 time period. Nonetheless, this analysis offers both a spatial and temporal climatological examination of the EWEs in the Ross Island vicinity, revealing peaks in EWE frequency during transition seasons and insignificant trends in extreme events from 1992 to 2013.

4. Dynamical analysis

The synoptic-scale conditions during McMurdo Station EWEs are examined using AMPS data and HYSPLIT forecast back trajectories. The top 12 events (Table 3) are used as case studies for this analysis. The prevailing wind direction during these EWEs is consistent with the findings in the previous sections (and prior studies), with all of the events exhibiting predominantly southerly flow. An example of one of these events (specifically, the one that occurred on 3 September 2003) is depicted in Fig. 6. The most notable features in this case, as in most EWE events, include the deep (<960 hPa) low pressure system impinging on the Ross Ice Shelf from the north, the strong pressure gradient

over the ice shelf to the south of the storm, and the ridging of the isobars to the south and southwest of Ross Island. Figure 7 shows the effect of these features at Pegasus North. The pressure, temperature, wind speed, and wind direction are plotted at 10-min intervals from 0000 UTC 3 September to 0330 UTC 5 September. The pressure drops around 25 hPa (Fig. 7a) while the wind speed increases to over 37 m s⁻¹ (Fig. 7b), and the wind direction is nearly constant from the south. The observed increase in temperature (Fig. 7a) is due to the circulation of warmer, maritime air around the approaching cyclone.

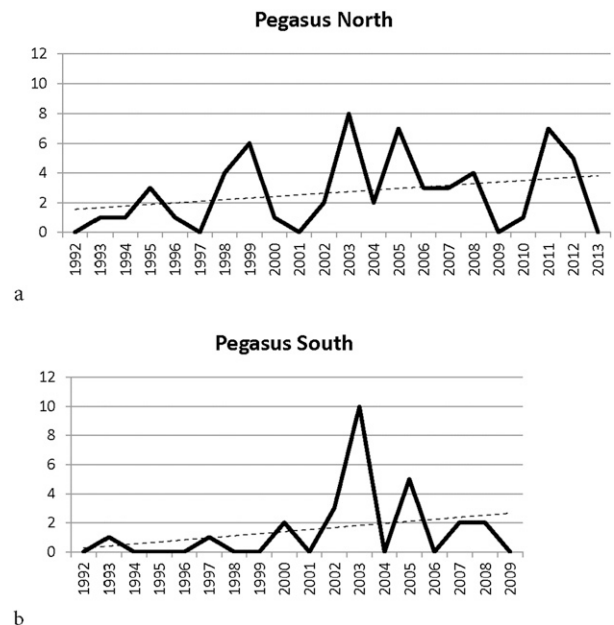


FIG. 5. Time series of the number of extreme wind events for (a) Pegasus North (1992–2013) and (b) Pegasus South (1992–2009). Dotted lines indicate the least squares linear trend.

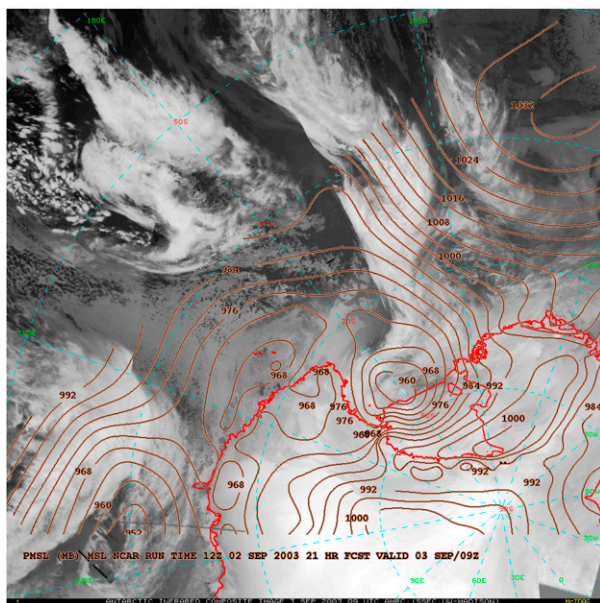


FIG. 6. Infrared satellite composite over the Ross Sea at 0900 UTC 3 Sep 2003 overlaid with AMPS mean sea level pressure (brown).

These synoptic-scale features depicted in Fig. 6 together contribute to the development of strong winds flowing parallel to the Transantarctic Mountains (the RAS). There is no apparent katabatic signal in the infrared imagery [as discussed in Bromwich (1989)], but there may still be a momentum contribution from downslope winds in the vicinity of Byrd, Mulock, and Skelton Glaciers. While Fig. 6 only depicts this single case, this synoptic structure is fairly representative of most EWEs. Before examining the EWE cases in further detail, a composite analysis is performed in order to assess the prevailing synoptic setup for these events.

The AMPS forecasts for each EWE (around the time of onset) are averaged together to provide a visualization of the synoptic conditions that are most prominent across all events (Fig. 8). The 500-hPa map (Fig. 8a) reveals that a deep upper-level trough north-northwest of the Ross Ice Shelf is a defining feature of these wind events. This trough is accompanied by a ridge on either side, with the eastern ridge over West Antarctica. At the surface, the ASL has migrated to a position much farther west than the mean climatological position (Fogt et al. 2012; Coggins and McDonald 2015) and been replaced by a high pressure ridge (Fig. 8b). The low pressure system is positioned so that the geostrophic winds intersect the Transantarctic Mountains orthogonally; this is a strong indicator of a barrier wind regime. The averaged surface fields for the area around McMurdo

Station and the Ross Ice Shelf (Figs. 8b–d) show the surface low in more detail. The barrier effect of the mountains builds high pressure along the range, as is evident in the ridging of the isohypses (O'Connor et al. 1994), which geostrophically forces a jet—or barrier wind—along the edge of the ice shelf toward Ross Island. The ground-level isotachs support this idea, revealing a jet along the Transantarctic Mountains (Fig. 8d) with a maximum average wind speed of roughly 20 m s^{-1} in the Ross Island vicinity. ERA-Interim composites of the 500-hPa height field and mean sea level pressure field for these 12 events (not shown) had very similar patterns compared to the AMPS composite fields, although the global reanalysis fields cannot fully show the details of the near-surface winds along the Transantarctic Mountains and around Ross Island. This composite analysis of the top 12 EWEs describes how the average event has a significant synoptic contribution from a Ross Sea cyclone and the barrier wind effect resulting from its orientation relative to the mountains; on average, EWEs are associated with a fairly well-defined RAS event. It is, however, likely that the contribution from different forcings (i.e., katabatic/downslope flow, barrier flow, or synoptic forcing) to the extreme winds at McMurdo Station varies from one case to another.

A more detailed examination of the EWEs represented in the top 12 McMurdo Station events is performed using the AMPS forecasts to compute back trajectories with HYSPLIT, which provide a Lagrangian perspective on these extreme wind regimes. HYSPLIT has been used successfully with the WRF Model previously (Stein et al. 2015). The AMPS-forecast back trajectories (Figs. 9a, 10a, and 11a) reveal several interesting patterns in the parcel paths leading up to these top EWEs at McMurdo Station. These forecast back trajectories have endpoints located at McMurdo Station. The endpoint heights included multiple levels at 10, 50, 100, and 500 m above ground level. Many of the EWE trajectories exhibit an RAS-like (barrier wind) structure, with flow approaching Ross Island from the south-southeast along the Transantarctic Mountains. Figure 9a shows the trajectories for the 23 May 2003 case. Strong surface flow stretches the length of the Transantarctic Mountains due to an intense low in the Ross Sea (Figs. 9c–e) with a deep trough at 500 hPa (Fig. 9b).

Other trajectories approach McMurdo Station from a more southwesterly direction at a very low elevation (Fig. 10a). The 20 September 2006 case is an example of this kind of situation. The surface pressure field has more of a trough than a closed low in the western Ross Sea (Figs. 10c–e), while the isotachs and wind barbs

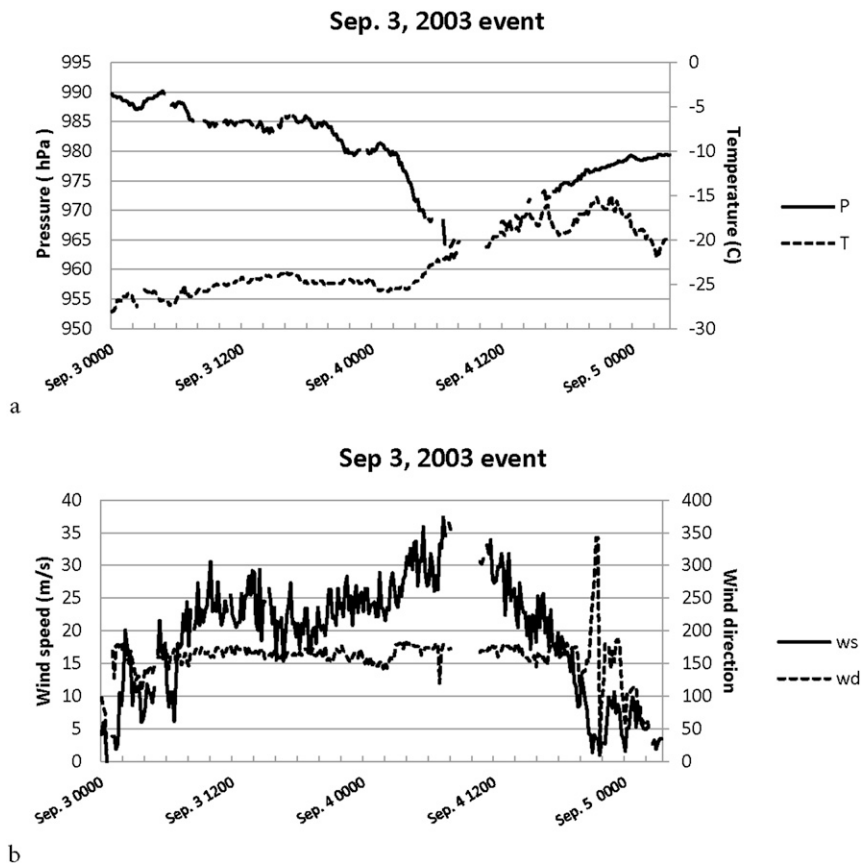


FIG. 7. Time series of (a) station pressure and temperature and (b) wind speed and wind direction for Pegasus North from 0000 UTC 3 Sep to 0330 UTC 5 Sep 2003, showing the effect of the extreme wind speed event that occurred on 3 Sep 2003.

point to some contribution to the flow in the vicinity of the Byrd, Mulock, and Skelton Glaciers, perhaps indicating a downslope flow. The 500-hPa height field (Fig. 10b) positions the upper-level trough farther away from the coast, and it is not as intense as in Fig. 9b. The trajectories in this case indicate that the air parcels did not all come from the same area. Air at different heights is being drawn into the system from different places as it flows down and around or over the topography.

A third pattern of back trajectories reveals a cyclonic spiraling pattern in the EWE parcel paths over the Ross Ice Shelf (Fig. 11a), as depicted by the 29 June 2005 case. The surface low is closer to Cape Adare and a wide band of strong winds flows the length of the Ross Ice Shelf and out into the Ross Sea (Figs. 11c–e). The 500-hPa heights have two large troughs on either side of the continent with the ridge over the Amundsen Sea area positioned farther off the coast (Fig. 11b).

Every trajectory indicates southerly or near-southerly flow at the onset of the EWE at Ross Island. Thus, it is

clear that the aforementioned low pressure over the Ross Ice Shelf, which generates this southerly flow, is a crucial ingredient for extreme winds at McMurdo Station. It is less clear how much of a contribution other forcings, such as katabatic or downslope winds, may have.

The back trajectories reveal that, despite the near ubiquity of the Ross Ice Shelf low investigated earlier, the EWE parcels exhibit a variety of behaviors from case to case. Looking back at the AMPS surface composite map (Figs. 8b,c), it can be seen that, in addition to the barrier-like jet along the mountains, there is a split in the local wind speed maximum with one branch over the McMurdo Station/McMurdo Sound and the other over the eastern tip of Ross Island, which is the outflow region for the RAS. The topography of Ross Island causes this split in the wind direction as the flow moves around both sides of the high terrain. The flow around the eastern side of Ross Island is similar to the tip jet effect described in Nigro et al. (2012), which increases the wind speed of the RAS. The flow over Hut Point Peninsula

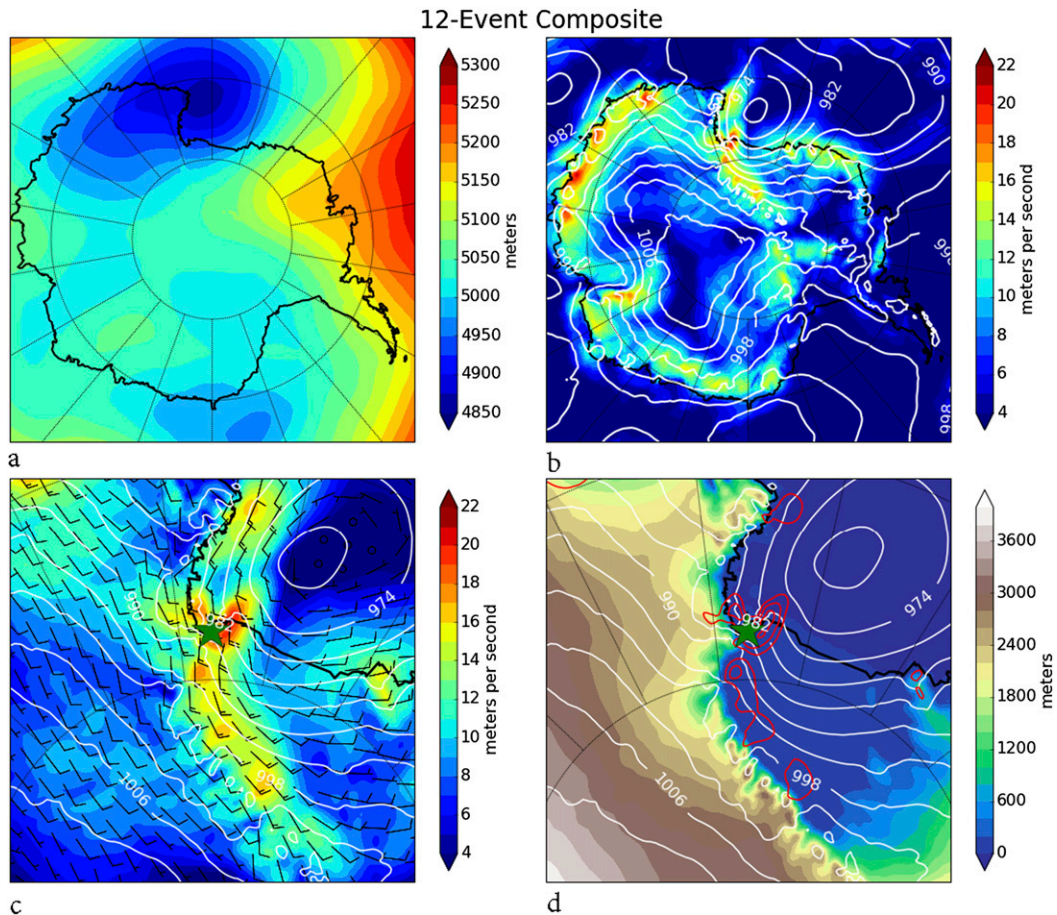


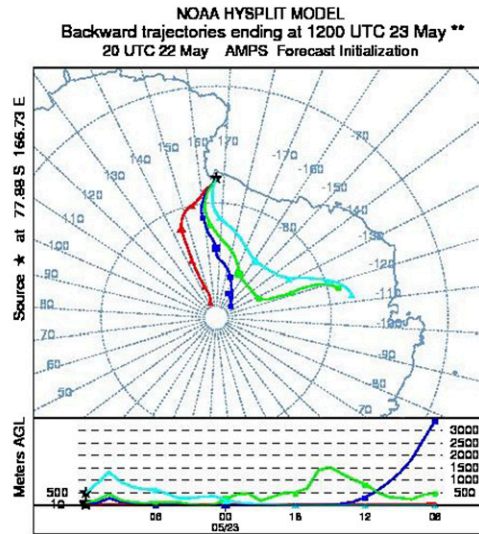
FIG. 8. Composite fields of the 12 highest wind speed events listed in Table 3: (a) 500-hPa heights (m); (b) surface wind speed (m s^{-1} ; shading) and mean sea level pressure (hPa; white contours); (c) surface wind speed (m s^{-1} ; shading), mean sea level pressure (hPa; white contours), and vector wind barbs around McMurdo Station; and (d) surface wind speed (m s^{-1} ; red contours with a 2 m s^{-1} interval starting at 15 m s^{-1}), mean sea level pressure (hPa; white contours), and terrain height (m; shading) around McMurdo Station.

and McMurdo Station is a reflection of the localized high pressure area that forms on the windward side of Ross Island (near Windless Bight) when high wind speeds impinge on the higher topography in this area (Seefeldt et al. 2003; Adams 2005; Chenoli et al. 2015). The flow is directed around and over Hut Point with an increase in speed due to the local pressure gradient created by mass accumulation along the Transantarctic range. Looking closely at Figs. 8b and 8c, there are also local wind speed maxima both at the outlet of the glaciers and in the lee of the topography upstream of Ross Island (Steinhoff et al. 2008), indicating some contribution from downslope flow off Byrd, Mulock, and Skelton Glaciers, just upstream of McMurdo Station (relative to the RAS). This idea is supported by several of the back trajectories discussed previously, which show the airstreams from the glaciers converging into a northward flow. While the synoptically forced RAS is crucial to the McMurdo

Station EWEs, there may also be a contribution from the downslope flow from nearby glaciers and/or flow around or over the local topography that can amplify the severity of these winds (Parish and Bromwich 2007).

5. Discussion

The position of the ASL and the associated trough at 500 hPa are crucial to the setup of conditions that bring extremely high wind events into the McMurdo area. The upper-level trough must be positioned farther to the west than normal so that surface cyclones are steered into the Ross Sea/Ross Ice Shelf area. Several large-scale features have a strong influence on the movement of the ASL and its associated trough at 500 hPa. The work of Fogt et al. (2012) describes the position of the ASL as determined mainly by the topography of Antarctica (the Antarctic Peninsula and the sloping terrain).



a

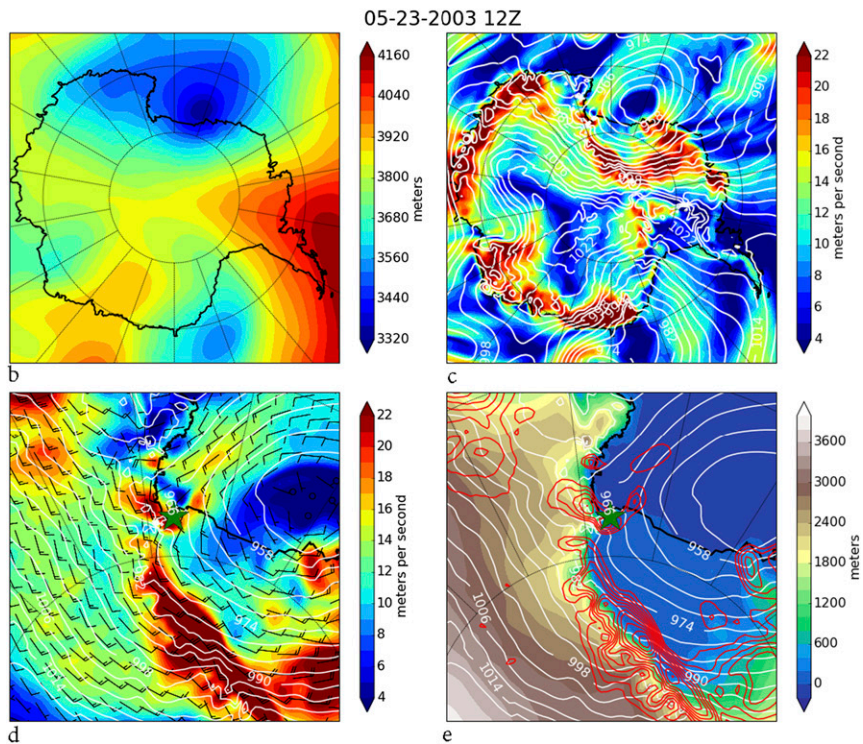


FIG. 9. (a) AMPS-fed HYSPLIT 3-day forecast back trajectories ending at McMurdo Station for the EWE starting on 23 May 2003. The four trajectory lines end at 10 (red), 50 (blue), 100 (green), and 500 (cyan) m AGL. (b) The 500-hPa heights (m). (c) Surface wind speed (m s^{-1} ; shading) and mean sea level pressure (hPa; white contours). (d) Surface wind speed (m s^{-1} ; shading), mean sea level pressure (hPa; white contours), and surface wind barbs. (e) Surface wind speed (m s^{-1} ; red contours with a 2 m s^{-1} interval starting at 15 m s^{-1}), mean sea level pressure (hPa; white contours), and terrain height (m; shading) around McMurdo Station.

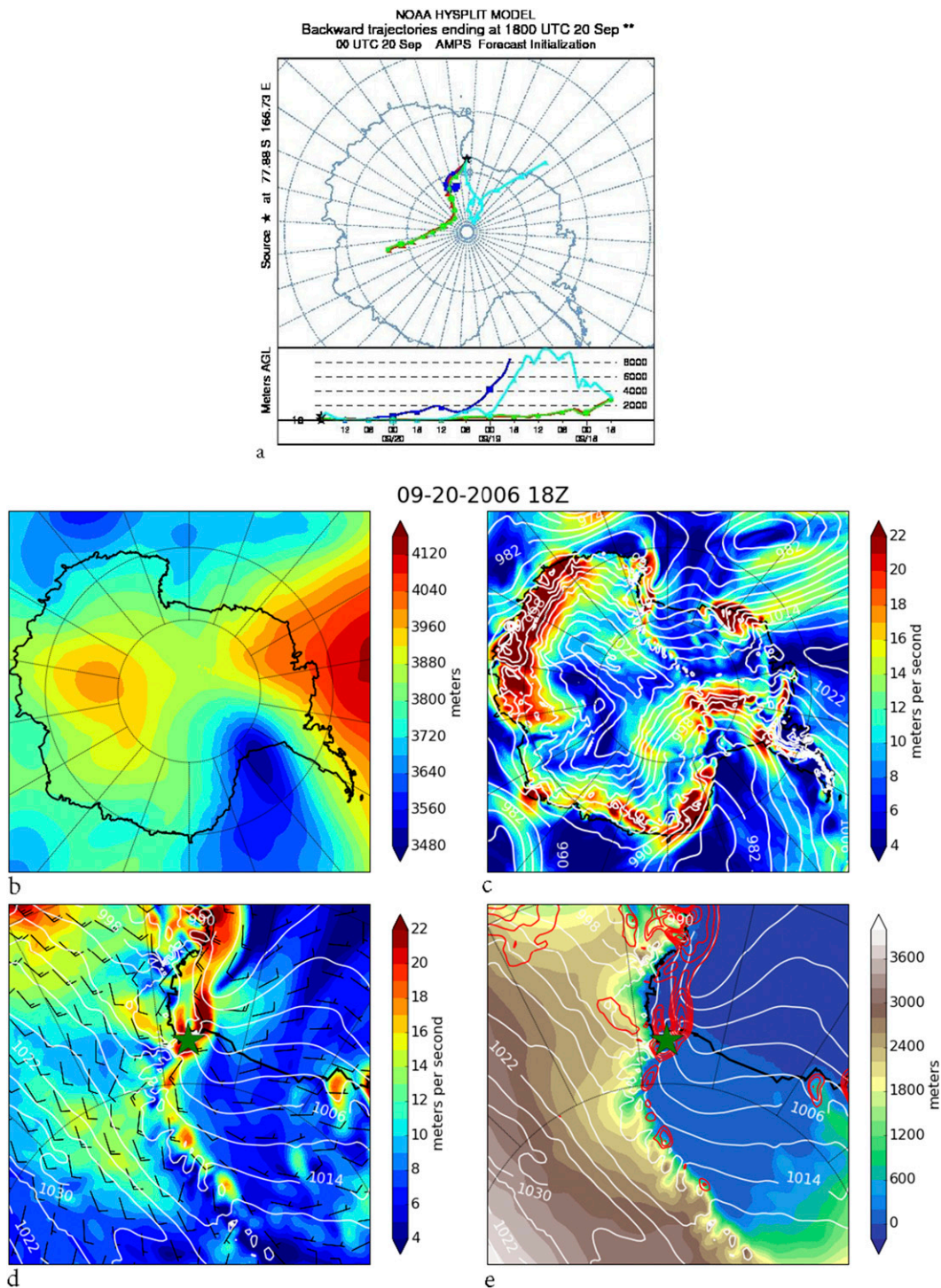


FIG. 10. As in Fig. 9, but for the EWE starting on 20 Sep 2006.

The center migrates to the west and south in fall and winter and to the east in summer. In addition to the topography, the position of the ASL is also influenced by the phase of the southern annular mode (SAM). A

positive phase of SAM is correlated with a strong low pressure system in the ASL region (Fogt et al. 2012). This would indicate that the possibility of a strong low pressure anomaly outside of the ASL area would be

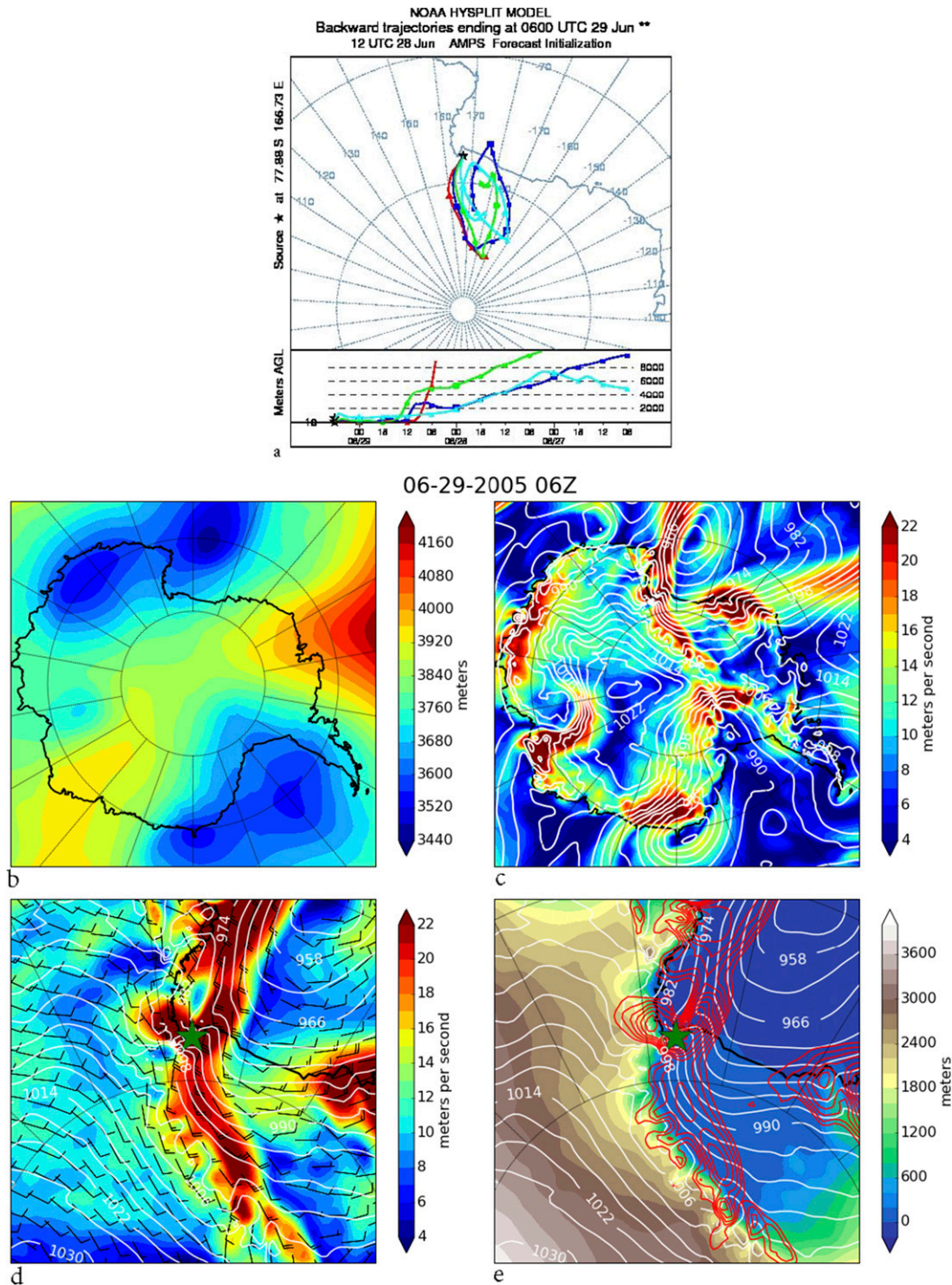


FIG. 11. As in Fig. 9, but for the EWE starting on 29 Jun 2005.

associated with a negative phase of SAM. Looking at the top 12 events discussed for the McMurdo area, 7 occur with a slightly negative phase of the SAM (events from 2003 to 2009). The first three events and last two events occur with a positive phase of SAM.

The phase of SAM does not appear to have a decisive influence on the possibility of EWEs at McMurdo Station.

Another large-scale feature that could influence the position of the cyclones is the semiannual oscillation, where the Antarctic circumpolar trough moves closest

to the continent in March and September (Van Loon 1967; Simmonds and Jones 1998). While this oscillation has its roots in the changing heating and cooling rates of the temperatures during the transition seasons, it may contribute to the bimodal distribution of the strong wind events studied by Chenoli et al. (2012). Since this study is looking at extreme events, there does not appear to be as great a connection, except for perhaps during September.

Neither of the above possibilities seems to explain the far western position of the ASL and associated upper-level trough, which is necessary for the extreme wind events to occur. The ENSO central Pacific (CP) events (Ashok et al. 2007, 2009; Kao and Yu 2009; Capotondi et al. 2015) are another possible explanation. With a CP El Niño, the Pacific–South American stationary wave pattern is shifted to the west with a high appearing in the Amundsen Sea area. The South Pacific convergence zone (SPCZ) is stronger in austral winter and is also shifted southwest (Wilson et al. 2014). Using the years defined by Wilson et al. (2014) as having CP events, eight of the EWEs described here occurred during CP El Niño events and four occurred during CP La Niña events. As this manuscript was being prepared, another EWE occurred at McMurdo Station in February 2015 during a CP El Niño event. While the CP ENSO events do not cause the EWEs to occur at McMurdo Station, they do appear to influence the position of the large-scale circulation in such a way that favors the occurrence of such events.

6. Conclusions

This study provides a statistical and dynamical examination of the top-tier wind events, or EWEs, at McMurdo Station in order to assess the behavior of these storms and how they might differ from typical strong wind events (SWEs) in the Ross Island region of Antarctica. The statistical analysis shows that EWEs tend to occur during the transitional seasons, perhaps because of the expansion and contraction of the circumpolar trough. Furthermore, there has been no statistically significant trend in the frequency, duration, or intensity of EWEs near McMurdo Station [consistent with the Chenoli et al. (2012) analysis of SWEs].

Our dynamical investigation reveals a great deal about the structure and behavior of these EWEs. First, these extreme events consistently produce southerly flow at McMurdo Station because of the large Froude number (Chenoli et al. 2012, 2015) associated with the high wind velocities that allow the air to pass over the topographical barriers. This distinguishes EWEs from SWEs, which have a bimodal wind direction distribution because the lower wind speeds cause the air to flow around rather than over the topography. Second, EWEs

are almost always associated with a low pressure system encroaching upon the Ross Ice Shelf from the north, northeast, or even the northwest. The presence of a deep trough of low pressure at 500 hPa in the vicinity or to the west of Cape Adare seems to be the key ingredient for this scenario (Coggins and McDonald 2015). Finally, the RAS regime created by this synoptic environment seems to be a necessary, but insufficient, ingredient for producing extreme winds at McMurdo Station. The southerly barrier flow in the Ross Island vicinity during these EWEs is likely enhanced by the tip jet effect, local pressure gradient forces due to topography, and/or downslope winds in the lee of Minna Bluff and Black and White Islands, all of which produces a local wind speed maximum in the McMurdo region. This further differentiates EWEs from SWEs, which can be produced by any of these forcings separately.

Forecasting these events does remain a challenge. The position of the 500-hPa trough and the encroachment of a surface cyclone are determining factors for the possibility of an EWE. The incidence of a CP ENSO event appears to be a favorable influence on the upper-level trough position so that an approaching surface cyclone would be more likely to trigger an event, depending on the angle of approach and the effect of the topography in the McMurdo Station area. Climate studies have shown that CP El Niño events are increasing in frequency (Ashok et al. 2007) and intensity (Lee and McPhaden 2010), which may increase the possibility of EWE events.

The insight gained about EWEs through this study has several implications for the communities at McMurdo Station and Scott Base. Knowing that the strongest events tend to occur in the transitional seasons can impact transportation and the length of the field season. Additionally, the knowledge that these events have southerly wind directions can aid in the design of McMurdo area structures.

Acknowledgments. Thanks are extended to D. J. Rasmussen for the data retrieval and analysis that formed the foundation of this study, and to Sam Batzli for the maps of the Ross Island area. The authors gratefully acknowledge the NOAA Air Resources Laboratory (ARL) for the provision of the HYSPLIT transport and dispersion model used in this publication. We also thank the two anonymous reviewers who helped us clarify and improve the paper. The authors appreciate the support of the Division of Polar Programs at the National Science Foundation, NSF Grants ANT-0944018, ANT-1043478, ANT-1141908, ANT-1245663, and ANT-1245737 in support of the U.S. Antarctic AWS Program and Antarctic Meteorological Research Center.

REFERENCES

- Adams, A. S., 2005: The relationship between topography and the Ross Ice Shelf air stream. Ph.D. dissertation, University of Wisconsin–Madison, 125 pp.
- Ashok, K., S. K. Behera, S. A. Rao, H. Weng, and T. Yamagata, 2007: El Niño Modoki and its possible teleconnection. *J. Geophys. Res.*, **112**, C11007, doi:10.1029/2006JC003798.
- , C.-Y. Tam, and W.-J. Lee, 2009: ENSO Modoki impact on the Southern Hemisphere storm track activity during extended austral winter. *Geophys. Res. Lett.*, **36**, L12705, doi:10.1029/2009GL038847.
- Bromwich, D. H., 1988: Snowfall in high southern latitudes. *Rev. Geophys.*, **26**, 149–168, doi:10.1029/RG026i001p00149.
- , 1989: Satellite analyses of Antarctic katabatic wind behavior. *Bull. Amer. Meteor. Soc.*, **70**, 738–749, doi:10.1175/1520-0477(1989)070<0738:SAOAKW>2.0.CO;2.
- , A. J. Monaghan, J. G. Powers, J. J. Cassano, H.-L. Wei, Y.-H. Kuo, and A. Pellegrini, 2003: Antarctic Mesoscale Prediction System (AMPS): A case study from the 2000–01 field season. *Mon. Wea. Rev.*, **131**, 412–434, doi:10.1175/1520-0493(2003)131<0412:AMPSAA>2.0.CO;2.
- , —, K. W. Manning, and J. G. Powers, 2005: Real-time forecasting for the Antarctic: An evaluation of the Antarctic Mesoscale Prediction System (AMPS). *Mon. Wea. Rev.*, **133**, 579–603, doi:10.1175/MWR-2881.1.
- Capotondi, A., and Coauthors, 2015: Understanding ENSO diversity. *Bull. Amer. Meteor. Soc.*, **96**, 921–938, doi:10.1175/BAMS-D-13-00117.1.
- Carrasco, J. F., and D. H. Bromwich, 1993: Mesoscale cyclogenesis dynamics over the southwestern Ross Sea, Antarctica. *J. Geophys. Res.*, **98**, 12 973–12 995, doi:10.1029/92JD02821.
- Chenoli, S. N., J. Turner, and A. A. Samah, 2012: A climatology of strong wind events at McMurdo Station, Antarctica. *Int. J. Climatol.*, **33**, 2667–2681, doi:10.1002/joc.3617.
- , —, and —, 2015: A strong wind event on the Ross Ice Shelf, Antarctica: A case study of scale interactions. *Mon. Wea. Rev.*, **143**, doi:10.1175/MWR-D-15-0002.1.
- Coggins, J. H. G., and A. McDonald, 2015: The influence of the Amundsen Sea low on the winds in the Ross Sea and surroundings: Insights from a synoptic climatology. *J. Geophys. Res. Atmos.*, **120**, 2167–2189, doi:10.1002/2014JD022830.
- Cohen, L., S. Dean, and J. Renwick, 2013: Synoptic weather types for the Ross Sea region, Antarctica. *J. Climate*, **26**, 636–649, doi:10.1175/JCLI-D-11-00690.1.
- Fogt, R. L., A. J. Wovrosh, R. A. Langen, and I. Simmonds, 2012: The characteristic variability and connection to the underlying synoptic activity of the Amundsen–Bellingshausen Seas low. *J. Geophys. Res.*, **117**, D07111, doi:10.1029/2011JD017337.
- Guo, Z., D. H. Bromwich, and J. J. Cassano, 2003: Evaluation of Polar MM5 simulations of Antarctic atmospheric circulation. *Mon. Wea. Rev.*, **131**, 384–411, doi:10.1175/1520-0493(2003)131<0384:EOPMSO>2.0.CO;2.
- Holmes, R. E., C. R. Stearns, G. A. Weidner, and L. M. Keller, 2000: Utilization of automatic weather station data for forecasting high wind speeds at Pegasus Runway, Antarctic. *Wea. Forecasting*, **15**, 137–151, doi:10.1175/1520-0434(2000)015<0137:UOAWSD>2.0.CO;2.
- Kao, H. Y., and J. Y. Yu, 2009: Contrasting eastern Pacific and central Pacific types of ENSO. *J. Climate*, **22**, 615–632, doi:10.1175/2008JCLI2309.1.
- Keller, L. M., G. A. Weidner, C. R. Stearns, M. T. Whittaker, and R. E. Holmes, 1996: Antarctic automatic weather station data for the calendar year 1994. Dept. of Atmospheric and Oceanic Sciences, University of Wisconsin–Madison, 465 pp. [Available from Antarctic Meteorological Research Center, Space Science and Engineering Center, University of Wisconsin–Madison, 1225 West Dayton St., Madison, WI 53706.]
- , —, —, —, and —, 1997: Antarctic automatic weather station data for the calendar year 1995. Dept. of Atmospheric and Oceanic Sciences, University of Wisconsin–Madison, 539 pp. [Available from Antarctic Meteorological Research Center, Space Science and Engineering Center, University of Wisconsin–Madison, 1225 West Dayton St., Madison, WI 53706.]
- King, J. C., and J. Turner, 1997: *Antarctic Meteorology and Climatology*. Cambridge University Press, 409 pp.
- Knuth, S. L., G. J. Tripoli, J. E. Thom, and G. A. Weidner, 2010: The influence of blowing snow and precipitation on snow depth change across the Ross Ice Shelf and Ross Sea regions of Antarctica. *J. Appl. Meteor. Climatol.*, **49**, 1306–1321, doi:10.1175/2010JAMC2245.1.
- Lazzara, M. A., G. A. Weidner, L. M. Keller, J. E. Thom, and J. J. Cassano, 2012: Antarctic Automatic Weather Station Program: 30 years of polar observations. *Bull. Amer. Meteor. Soc.*, **93**, 1519–1537, doi:10.1175/BAMS-D-11-00015.1.
- Lee, T., and M. J. McPhaden, 2010: Increasing intensity of El Niño in the central-equatorial Pacific. *Geophys. Res. Lett.*, **37**, L14603, doi:10.1029/2010GL044007.
- Markle, B. R., N. A. N. Bertler, K. E. Sinclair, and S. B. Sneed, 2012: Synoptic variability in the Ross Sea region, Antarctica, as seen from back-trajectory modeling and ice core analysis. *J. Geophys. Res.*, **117**, D02113, doi:10.1029/2011JD016437.
- Monaghan, A. J., D. H. Bromwich, J. G. Powers, and K. W. Manning, 2005: The climate of the McMurdo, Antarctic, region as represented by one year of forecasts from the Antarctic Mesoscale Prediction System. *J. Climate*, **18**, 1174–1189, doi:10.1175/JCLI3336.1.
- Murphy, B. F., 2003: Prediction of severe synoptic events in coastal East Antarctica. *Mon. Wea. Rev.*, **131**, 354–370, doi:10.1175/1520-0493(2003)131<0354:POSSEI>2.0.CO;2.
- , and I. Simmonds, 1993: An analysis of strong wind events simulated in a GCM near Casey in the Antarctic. *Mon. Wea. Rev.*, **121**, 522–534, doi:10.1175/1520-0493(1993)121<0522:AAOSWE>2.0.CO;2.
- Nigro, M. A., and J. J. Cassano, 2014a: Identification of surface wind patterns over the Ross Ice Shelf, Antarctica, using self-organizing maps. *Mon. Wea. Rev.*, **142**, 2361–2378, doi:10.1175/MWR-D-13-00382.1.
- , and —, 2014b: Analysis of the Ross Ice Shelf airstream forcing mechanisms using self-organizing maps. *Mon. Wea. Rev.*, **142**, 4719–4734, doi:10.1175/MWR-D-14-00077.1.
- , —, M. A. Lazzara, and L. M. Keller, 2012: Case study of a barrier wind corner jet off the coast of the Prince Olav Mountains, Antarctica. *Mon. Wea. Rev.*, **140**, 2044–2063, doi:10.1175/MWR-D-11-00261.1.
- O’Connor, W. P., D. H. Bromwich, and J. F. Carrasco, 1994: Cyclonically forced barrier winds along the Transantarctic Mountains near Ross Island. *Mon. Wea. Rev.*, **122**, 137–150, doi:10.1175/1520-0493(1994)122<0137:CFBWAT>2.0.CO;2.
- Parish, T. R., and D. H. Bromwich, 1998: A case study of Antarctic katabatic wind interaction with large-scale forcing. *Mon. Wea. Rev.*, **126**, 199–209, doi:10.1175/1520-0493(1998)126<0199:ACSOAK>2.0.CO;2.

- , and —, 2007: Reexamination of the near-surface airflow over the Antarctic continent and implications on atmospheric circulations at high southern latitudes. *Mon. Wea. Rev.*, **135**, 1961–1973, doi:[10.1175/MWR3374.1](https://doi.org/10.1175/MWR3374.1).
- , J. J. Cassano, and M. W. Seefeldt, 2006: Characteristics of the Ross Ice Shelf air stream as depicted in Antarctic Mesoscale Prediction System simulations. *J. Geophys. Res.*, **111**, D12109, doi:[10.1029/2005JD006185](https://doi.org/10.1029/2005JD006185).
- Powers, J. G., 2007: Numerical prediction of an Antarctic strong wind event with the Weather Research and Forecasting (WRF) Model. *Mon. Wea. Rev.*, **135**, 3134–3157, doi:[10.1175/MWR3459.1](https://doi.org/10.1175/MWR3459.1).
- , K. W. Manning, D. H. Bromwich, J. J. Cassano, and A. M. Cayette, 2012: A decade of Antarctic science support through AMPS. *Bull. Amer. Meteor. Soc.*, **93**, 1699–1712, doi:[10.1175/BAMS-D-11-00186.1](https://doi.org/10.1175/BAMS-D-11-00186.1).
- Schwerdtfeger, W., 1984: *Weather and Climate of the Antarctic*. Developments in Atmospheric Science, Vol. 15, Elsevier Science, 262 pp.
- Seefeldt, M. W., G. J. Tripoli, and C. R. Stearns, 2003: A high-resolution numerical simulation of the wind flow in the Ross Island region, Antarctica. *Mon. Wea. Rev.*, **131**, 435–458, doi:[10.1175/1520-0493\(2003\)131<0435:AHRNSO>2.0.CO;2](https://doi.org/10.1175/1520-0493(2003)131<0435:AHRNSO>2.0.CO;2).
- , J. J. Cassano, and T. R. Parish, 2007: Dominant regimes of the Ross Ice Shelf wind field during austral autumn 2005. *J. Appl. Meteor. Climatol.*, **46**, 1933–1955, doi:[10.1175/2007JAMC1442.1](https://doi.org/10.1175/2007JAMC1442.1).
- Simmonds, I., and D. A. Jones, 1998: The mean structure and temporal variability of the semiannual oscillation in the southern extratropics. *Int. J. Climatol.*, **18**, 473–504, doi:[10.1002/\(SICI\)1097-0088\(199804\)18:5<473::AID-JOC266>3.0.CO;2-0](https://doi.org/10.1002/(SICI)1097-0088(199804)18:5<473::AID-JOC266>3.0.CO;2-0).
- Stein, A. F., R. R. Draxler, G. D. Rolph, B. J. B. Stunder, M. D. Cohen, and F. Ngan, 2015: NOAA's HYSPLIT atmospheric transport and dispersion modeling system. *Bull. Amer. Meteor. Soc.*, **96**, 2059–2077, doi:[10.1175/BAMS-D-14-00110.1](https://doi.org/10.1175/BAMS-D-14-00110.1).
- Steinhoff, D. F., D. H. Bromwich, M. Lambertson, S. L. Knuth, and M. A. Lazzara, 2008: A dynamical investigation of the May 2004 McMurdo Antarctic severe wind event using AMPS. *Mon. Wea. Rev.*, **136**, 7–26, doi:[10.1175/2007MWR1999.1](https://doi.org/10.1175/2007MWR1999.1).
- , S. Chaudhuri, and D. H. Bromwich, 2009: A case study of a Ross Ice Shelf airstream event: A new perspective. *Mon. Wea. Rev.*, **137**, 4030–4046, doi:[10.1175/2009MWR2880.1](https://doi.org/10.1175/2009MWR2880.1).
- Turner, J., S. N. Chenoli, A. A. Samah, G. Marshall, T. Phillips, and A. Orr, 2009: Strong wind events in the Antarctic. *J. Geophys. Res.*, **114**, D18103, doi:[10.1029/2008JD011642](https://doi.org/10.1029/2008JD011642).
- Van Loon, H., 1967: The half-yearly oscillations in middle and high southern latitudes and the coreless winter. *J. Atmos. Sci.*, **24**, 472–486, doi:[10.1175/1520-0469\(1967\)024<0472:THYOIM>2.0.CO;2](https://doi.org/10.1175/1520-0469(1967)024<0472:THYOIM>2.0.CO;2).
- Wilson, A. B., D. H. Bromwich, K. M. Hines, and S.-H. Wang, 2014: El Niño flavors and their simulated impacts on atmospheric circulation in the high southern latitudes. *J. Climate*, **27**, 8934–8955, doi:[10.1175/JCLI-D-14-00296.1](https://doi.org/10.1175/JCLI-D-14-00296.1).